Proceedings of the ASME 2010 3rd Joint US-European Fluids Engineering Summer Meeting and 8th International Conference on Nanochannels, Microchannels, and Minichannels
FEDSM-ICNMM2010
August 1-5, 2010, Montreal, Canada

FEDSM-ICNMM2010-30165

MICROFLUIDICALLY RECONFIGURABLE PHOTONICS AND MATTER

David Erickson

Department of Mechanical and Aerospace Engineering, Cornell University, Ithaca, New York, 14853 de54@cornell.edu.

ABSTRACT

In this talk I will describe our research into the use of microfluidics for enabling reconfigurability of photonic systems and matter itself. In the first of these systems it is well known that optical devices which incorporate liquids as a fundamental part of the structure can be traced at least as far back as the 18th century where rotating pools of mercury were proposed as a simple technique to create smooth mirrors for use in reflecting telescopes. The development of modern microfluidic and nanofluidic devices has enabled a present day equivalent of such devices centered on the marriage of fluidics and optics which we refer to as "Optofluidics." I will demonstrate here the fundamental advantages of using microfluidics to create adaptable photonic materials and provide a few specific examples related to fluid based optical switches. In the second aspect I will introduce how we use microfluidics to create dynamically programmable self-assembling materials, or programmable matter. The uniqueness of the approach I will demonstrate is that it uses dynamically-switchable affinities between assembling components facilitating the assembly of irregular structures.

INTRODUCTION

Reconfigurable systems are those in which some or all of a system's physical, chemical or electrical properties can be changed either on-command to enhance functionality or autonomously in response to a change in external/internal conditions. Such systems are ubiquitous in nature and have recently been realized in a wide range of engineering applications including self-healing polymers [1], self-reproducing [2] and dynamically reconfigurable [3] robots, morphing aircraft [4, 5], computing [6, 7] and adaptive space structures [8].

To help put the advantages of these systems in context, consider the field of electronics where the ubiquitous reconfigurable system is the Field Programmable Gate Array (FPGA) [9, 10]. Put simply, an FPGA is a semiconductor device that can be reprogrammed by the user at any time post-fabrication to perform any arbitrary set of logical functions. Such devices have brought forth a number of technological benefits including: *Cost* - in cases where relatively few pieces are required it is much cheaper to purchase and program off-the-shelf FPGAs than design an application specific integrated circuit, *Autonomy and Adaptability* – the operation of the chip can be repurposed or optimized on-the-fly at the whim of the user or as a result of changes in local conditions, *Robustness* – the system can compensate for local flaws that occur during manufacturing or as a result of use, and *Security* - FPGAs can be designed to self-erase the programmed circuitry making it difficult to reverse engineer captured devices. Despite the advantages demonstrated in electronics, in **almost no other field of chip-based technology (e.g. photonics, microfluidics) have equivalently ubiquitous reconfigurability techniques been developed.**

Due to space limitations, here I will focus on the two areas into which we are performing research related to reconfigurable matter and will save my discussion of reconfigurable photonics for the talk. The goal of the first direction below was to develop a better experimental understanding of the fluid-dynamical and fluid-structural processes involved in 3D cube assembly processes. In the second direction our goal is the development of two forms of thermorheologically enabled programmable matter systems.

FLUID DYNAMICS OF PROGRAMMABLE MATTER

As I describe below, our research conducted in this area is separated into 3 different subcategories. The first of these describes the assembly chamber and the docking procedure we developed based on the experimental and numerical results obtained under earlier work [11, 12]. The second section describes our work on developing of an optimal fluid structure interaction system that promotes cube alignment and docking. This was largely done by investigating different cube topologies and finding better ways of manipulating the fluidic conditions during assembly. ***We demonstrate in that section a robust procedure for obtaining perfect docking and alignment of cubes.*** The final section describes some of the quantitative results we have obtained including the ability to dock in the

proper upright orientation over 80% of the time and median assembly rates of 5s/block.

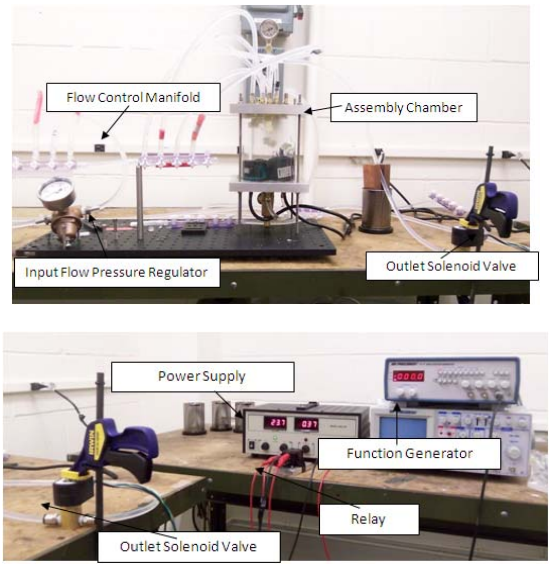

***Figure 1* – Erickson Lab Programmable Matter Apparatus for studying the Dynamics of the Assembly Process.** (Upper) Image shows overview of assembly chamber and associated infrastructure. Note the two circulation pumps at the bottom of the assembly chamber. The two pumps dramatically facilitate the generation of random motions within the tank. (Lower) Image shows electrical infrastructure associated with driving the solonoid valve. As will be demonstrated below the incorperation of an solonoid valve operating at 3 hz during the attraction process enables us to obtain proper docking.

Improvements to the assembly chamber and procedure.

A 3D assembly experimental setup has been developed in the Erickson Lab in order to facilitate study of cube docking and alignment. The setup is shown in Figure 1. The assembly chamber is similar to that which has been previously demonstrated however we now incorporate two major modifications which have been found to dramatically improve the docking rate and cube alignment during docking. As can be seen in the upper image of Figure 1 the bottom of the assembly chamber contains two circulation pumps (essentially fishtank circulation pumps) which provide a continuous swirl of fluid motion around the chamber without requiring very high input/output flow rates through the chamber. This reduced the required cube attraction pressure drop to below 2PSI which is something that can be easily modulated with thermorheological valves. The second major advancement was the incorporation of a single solenoid valve that controls the outlet flow from the chamber through the assembled structure. As will be expanded on in the next section, this allows for pulsation of the flow through the sink and increases the number of collisions that a new cube has with the previously assembled structure allowing it to settle down into its properly docked position.

Development of an optimal fluid structure interaction system that promotes cube alignment and docking.

The first experiments we conducted using the assembly chamber described above are shown in Figure 2 below. These cubes were unevenly weighted cubes which have a buoyancy driven preferred orientation during assembly (the sliver line at the top of the cubes shows the light end). This is done to reduce the number of degrees of freedom during docking. The left image in Figure 2 shows an example of an assembly event where the cube did dock properly (with the lighted part up) and the right image shows a case where it did not. ***We will expand on this in section 2.1.3 but the orientation assembly success rate was 84% using this lighted block technique.***

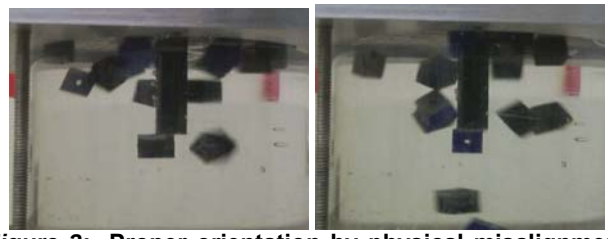

***Figure 2:* Proper orientation by physical misalignment during docking using initial square cubes.** Right image shows a block which has docked in the proper orientation (sliver line up) and the left image shows one which did not. In both cases however with purely square cubes, proper alignment does not occur. This result is directly predicted from simulation.

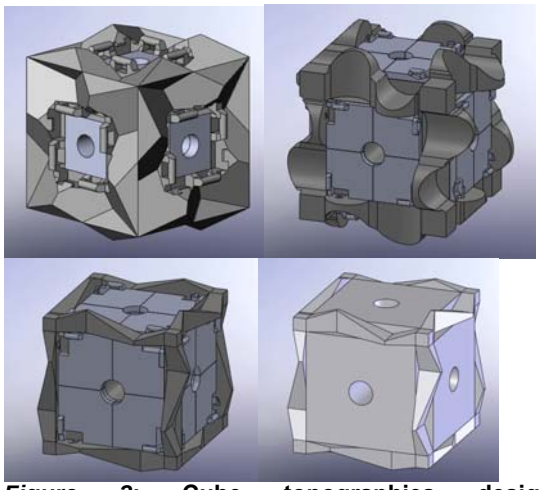

***Figure 3*: Cube topographies designed, manufactured and tested.** The cube in the top right corner represents the final design used below.

As can be seen from Figure 2 while the orientation is correct most times the alignment of new cubes added to the structure is mostly not correct (a clear offset is shown in both images of the Figure). In order to solve this problem a cube topography had to be developed that would (1) guide the assembly into place if docking is close (2) become stably latched to the structure upon contact (3) be able to be rejected upon reversal of the flow. Towards this end, several cube topographies were designed, manufactured and tested in the assembly chamber. Solid works files showing some of the cube designs that were tested are

shown in Figure 3. This extensive experimentation revealed that the cube design shown in the upper left hand corner yielded the best results.

Generally speaking however it was found that simply optimizing the cube topography was not enough to ensure robust docking of the cubes onto a structure. A typical result is shown in image 1 of Figure 4. As can be seen the cubes tended to dock with better alignment that the square cubes shown above but neither precise docking or latching could be obtained. To enable this we developed a "sink-cycling" technique which performed the final fluidic alignment after initial docking. Briefly, after initial docking was observed external valves on the chamber were switched so at to ensure most of the chamber flow was directed through the structure (rather than being used to promote chamber mixing (image 2 of Figure 4). Simultaneously with this a solenoid valve which controls the exit flow through the chamber was engaged at 3 hz with a 50% duty cycle (so the attraction flow through the structure was turned on and off 3 times a second half of the time on and half of the time off) using a function generator. It was found that this cycling motion (image 3 in Figure 4) served to "bounce" the cube into the properly docked position (image 4 in Figure 4). Attracted cubes could be aligned and docked approximately 70% of the time (i.e. 30% of cubes attracted to the pedestal had to be rejected). ***This represents an important advancement for us as it demonstrates a repeatable technique through which docking misalignments can be corrected.*** We expect that 70% alignment value could be greatly improved as the technique is optimized.

1) Cube attracted to pedastel but misaligned

2) After docking full suction is applied at the attraction point (convective flow turned off)

3) Attraction cycled by turning attraction pressure on-and-off using solonoid valve on exit line.

4) After several sections cube finds most stable point (alignment) and becomes fully docked.

Figure 4: **Docking and proper alignment of cube using suction enhancement and solonoid based sink-cycling.** Cube shown in image is the one from the upper right corner of Figure 1.

In addition to enabling the docking the "sink-cycling" technique was also sufficiently strong to promote latching between the cube and the structure. The latch design can be seen Figure 3 however in the actual implementation shown in Figure 3 we used only 2 latches per face (so four total latching interactions). The smaller number of latches allowed us to maintain sufficient strength so that the structure was stable but was still sufficient weak that reversing the flow enabled one to reject the cube from the structure (as shown in Figure 5). ***This was critically important because it demonstrates our concept of structural error correction.***

(a) t =0 s

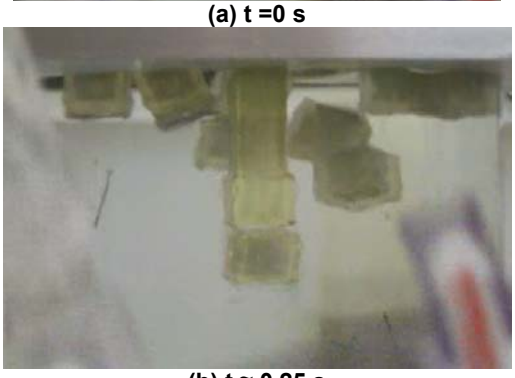

(b) t ≈ 0.25 s

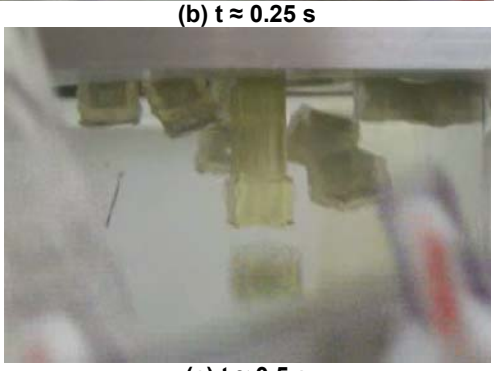

(c) t ≈ 0.5 s

Figure 5: **Time lapse images a cube being released from the docked position**: (a) initially, there is now flow in/out of the docking pedestal at t = 0 s flow out of the pedestal is initiated; (b) the flow rejects the block; (c) the blocks moves out into the bulk flow.

Figure 6 below illustrates a mock up of the initial target structures we will build with the assembly tank. By selectively plugging some of the holes in the structures we can pre-valve them (while the "smart cubes" are being developed) and assembly multi-cube structures like the C & U structures shown in the figure. ***We note that the latches on the structures are sufficiently strong that they can support the weight of the structure after the assembly fluid is drained.***

***Figure 6*: Docking and proper alignment of cube using suction enhancement and solonoid based sink-cycling.** Cube shown in image is the one from the upper right corner of Figure 1.

Initial results for docking time probabilities and alignment successes.

In Figure 7 we show a histogram of the average docking time, or the time between assembly events for the 3D cubes. As can be seen the average docking time for the cubes using the chamber above was 11s. ***As can also be seen in half of the 24 trials the assembly time was less than 5 seconds.*** Additionally, as mentioned above, 20 out of 24 cubes docked with the proper buoyancy corrected alignment. The amounted to a 84% orientation efficiency.

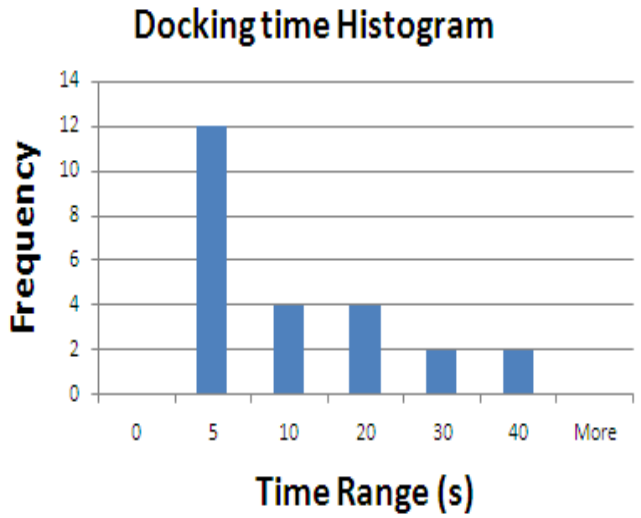

***Figure 7*: Histogram of docking times.** The average docking time for the cubes was 11s. In half of the 24 trials it took less than 5s for docking to occur.

THERMO-RHEOLOGICAL PROGRAMMABLE MATTER

The second area of research we are performing is on the development of the thermo-optically programmable surfaces and assemblies. In the below I focus on the accomplishments related to direct optical control the mechanical properties of a thermo-rheological fluid using the technique illustrated in Figure 8. In the below we show the capability to dynamically modulate the properties of the fluid from liquid to solid on time scales of less than 1s using only low intensity light. As shown in Figure 8 the basic premise is that light is shined on a surface which contains a photothermal conversion layer (various types of light absorbing layers are used below) which converts the light to heat and locally gels up the fluid. In this section we report the results in the context of developing a technique for dynamically reconfigurable microfluidics. After that we report further results relating this work to the assembly of 2D tiles. In both this section and section 3.0 the thermorheological fluid used in our experiments here is a 15% (w/w) aqueous solution of Pluronic F127 (BASF) with a gelation temperature of approximately 30 °C.

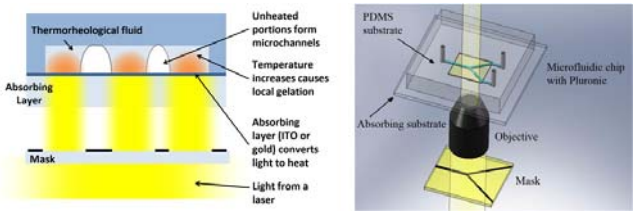

***Figure 8* – Overview of envisioned thermooptically programmable materials.** Left image shows experimental arrangement and process by which optically triggered spatial distributions in gellation (and hence material properties) occur. Right image shows 3D overview of technique.

Demonstration of thermooptically controlled flow and localized gelling

As mentioned above, the first set of experiments we conducted towards developing the thermooptically programmable material described above were aimed at characterizing the optical conditions which would lead to localized gelation. A schematic describing the apparatus used to conduct these experiments is shown in Fig. 9. The microfluidic chip we used consisted of an upper part containing a patterned microchannel that is bonded to a substrate with a coating on it that absorbs light. Analogous to what is shown in Figure 8 by selectively illuminating the absorbing substrate with a laser light, we are able to convert the optical energy to thermal energy and gel the thermorheological fluid flowing in the channel.

To demonstrate the effect we performed "Opto-thermorheological" valving in a T-shaped microfluidic channel as shown in Figure 9. Initially, the flow rate through each of the bifurcating channels was the same. On illuminating one of the channels with laser light (405 nm, 40 mW power) through a 20X objective, we were able to reduce and eventually stop the flow in this channel and direct all the flow into the other one as shown in Figure 10(a). The same objective was also used to image the sample, and the flow was visualized by seeding the fluid with 1.5 μm silica particles (Duke Scientific). As shown in Figure 10(b), when a non-absorbing plain glass substrate was used, no such gellation or valving was observed. The insets in each image of the figure show a zoomed up view of flow velocity in the valved channel. The microfluidic channels used here were fabricated using standard soft lithography techniques with poly(dimethylsiloxane) (PDMS) (Ellsworth Adhesives).

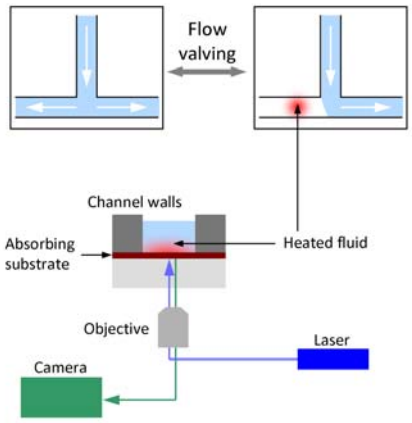

***Figure 9* – Schematic demonstrating valving technique with a laser and a microfluidic chip with an absorbing substrate.**

We used two different kinds of absorbing substrates for these experiments; a plain glass substrate with gold sputter deposited on it and a cover slip coated with indium tin oxide (ITO) (Sigma-Aldrich) as well as a non-absorbing plain glass substrate for control experiments. We also looked at the effect of varying channel width on the valving and considered channels of widths 25 and 50 μm. The height of the channels was kept constant at 25 μm. The results in Figure 10(a) are for an ITO coated substrate with a channel width of 50 μm, though we saw similar results for our other chips as well. Further details on these experiments are provided in our recent paper [13].

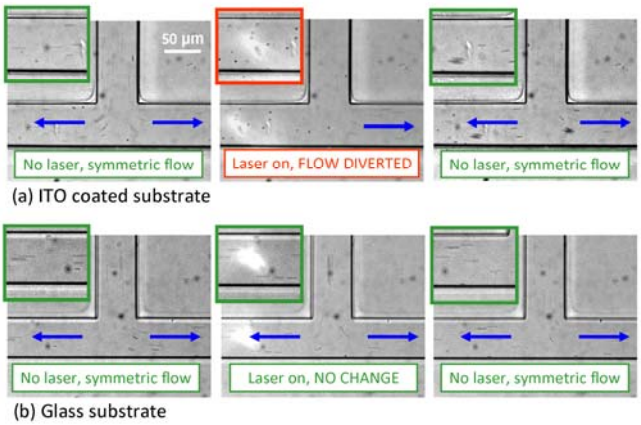

***Figure 10* – Demonstration of valving in a microfluidic channel (Media 1)** (a) ITO coated substrate (valving occurs). (b) Plain glass substrate (no valving).

To characterize the temperature rise at the gellation point, in situ temperature measurements using Rhodamine B were also carried for different channel geometries and substrates as described in [13]. The results here do indicate channel temperatures on the order of the sol-gel transition temperature; however we found that flow in the valved channel was not completely stopped. We expect this is because the yield stress of the gel formed in the channel is not sufficient to fully withstand the applied pressure. We attempted to improve the flow valving by increasing the beam power as well as changing the beam waist by using different magnification objectives, but found that higher beam powers and smaller beam waists resulted in bubble formation due to evaporation while larger beam waists resulted in too little heating and no subsequent gelation. These temperature measurements also show that the ITO coated substrate had higher temperatures over a wider region of the channel compared to the gold coated substrate. This indicates that the absorption of the ITO coated substrate is better than that of the sputtered gold substrate at the wavelength used in our experiments here (405 nm). We also found that the 25 μm channel with the ITO coated substrate had a higher temperature compared to the corresponding 50 μm channel which we expect is due to the lower thermal conductivity of the PDMS sidewalls compared to the aqueous pluronic solution in the channel (about 0.18 W/mK for PDMS compared to about 0.6 W/mK for water).

Directed assembly of programmable matter surfaces with hydrodynamically switchable affinities.

Self-assembly [14, 15] has been used to create structures at the micro- and nanoscales using techniques such as chemical bonding [16-18], fluid and surface tension based attraction [19-23], geometric interactions [24, 25] and magnetic fields [26, 27] as the assembly driving mechanism. Most of these self-assembly processes create either highly regular structures such as colloidal crystals [28], or small scale complex structures comprised of, for example, DNA polymers[29]. Recently Chung *et al.*[23] have developed a guided fluidic self-assembly process that allows for the assembly of relatively large irregular

structures. Using this technique, the authors were able to design the assembling components on-the-fly and transport them on a railed network to the assembly site. While this technique is very flexible in the shape of the components, their motion is confined by the pre-defined rail networks on which these components move.

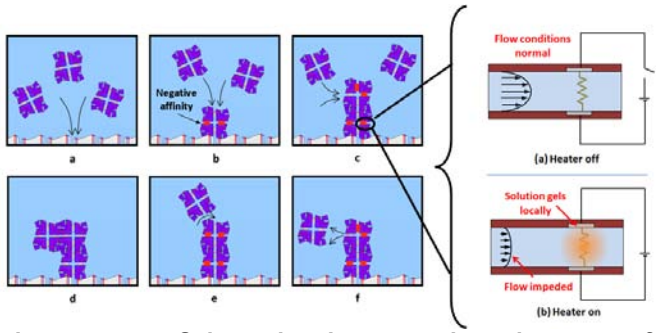

***Figure 11* – Schematic demonstrating the use of dynamically tunable affinities to create arbitrary, programmable and reconfigurable structures.** (a) shows the attraction of a sub-element moving stochastically in the fluid to the substrate. The sub-elements are unpowered while in the fluid, but once they are attached to the substrate they can draw power to switch their affinities. (b), (c) depict the building of an arbitrary target structure by dynamically switching the affinities within the structure and controlling the local attraction basin around the structure. (d) shows the final assembled structure. (e) shows reconfiguration of the assembled structure by switching affinities. (f) shows error correction to reject an incorrectly assembled component. INSET: Inset shows image of flow valving using a thermorheological fluid (a) off state (b) on state.

A hurdle to exploiting the potential of self-assembly is the inability of current techniques to assemble complex structures comprising large numbers of particles in non-regular, non-predefined geometries. One of the reasons for this is the use of static interactions, or *affinities* between the assembling components to drive the assembly process. For example, in nucleic-acid driven assembly, the final structure is governed by the predefined base-pair sequence [16, 30]. As a result, the assembling components and their affinities need to be specifically designed *a priori* for a given target structure. Since each affinity sequence corresponds to a specific target structure, assembled structures are also not generally reconfigurable. Similar arguments can be made for many hydrophobic/hydrophilic[20, 21, 31] and geometric/surface tension interactions[24, 25]. One way to address the above issues is to develop a means to dynamically (*i.e.* during assembly) tune affinities between assembling components. The concept of affinity switching has been demonstrated at the centimeter scale using mechanical and magnetic switching [32-36]. These methods however are difficult to implement at the microscale due to fabrication constraints and energy limitations.

The 3rd area of research we are pursuing is related to the development of programmable matter surfaces which exploit hydrodynamically tunable affinity switching. This builds on the initial silicon tile work we have recently published [12, 37]. Our process for affinity switching is shown in the schematic in Figure 11. In the process, locally restricting the flow near one face of the structure limits the probability of another component being attracted to that face. Hence that part of the structure has no affinity for an approaching component, while other parts of the structure are still positive affinity regions. Figure 11 shows the use of affinity switching by flow modulation to create irregular structures, reconfigure structures and carry out error correction. Each of these moves was demonstrated using 2D silicon tiles in the previous report. We note that this affinity switching process is the same as the technique currently being used in 3D and the results obtained here are equivalently transferable to that work.

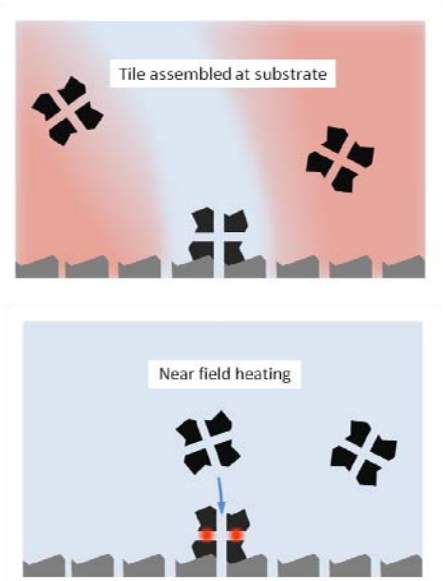

***Figure 12* – Thermorheological control of assembly process for both** (a) Far-field directed assembly and (b) near field directed assembly.

Here we report the development of the technique for manufacturing the tiles with embedded microchannels and to come up with a technique for assembling an arbitrary structure from them. The basic assembly strategy we intend to follow is shown in Figure 12 and provides one of the main motivations for pursuing the opto-thermorheologically modulated material system described above. As shown in Figure 12 we intend here to use a DMD system to direct both the far field directed assembly (left image) of the tiles and perform the near field affinity tuning (right image). As is shown through global heating of the fluid we can create temporary "tracks" through which the tile motion of the assembly elements can be guided and through local heating in the embedded channels we can perform the affinity tuning. Although we plan to initially focus on demonstrating this in 2D, this technique could also be extended to 3D assembly.

A number of fabrication techniques were developed and tested. For these initial experiments we have decided to use polymer based tiles, rather than silicon ones as was done in the previous experiments, to facilitate the fabrication. The final procedure we decided on is shown in Figure 13. The 3-D tile structure was fabricated by stacking three layer consisting of lower SU-8, HFE-processable negative tone photoresist, and top SU-8. First, the silicon wafer was coated with OmnicoatTM at 3000 rpm and 200°C for 1 min prior to applying the SU-8 resist. The OmniCoat™ was used as a SU8 release layer. Following this,

the 20 μm thick SU-8 was spun at 4000 rpm for 30 s. The coated wafer was exposed to 120 mJ/cm^2 of contact aligner through a bottom-layer mask of the 3-D tile. After post-baking, it was dip developing solution for 60 s, rinsed in a IPA(isopropyl alcohol), and dried with N_2 gas. To improve the adhesion between second layer (HFE-processable negative tone photoresist) and SU-8 layer, the wafer was activated with oxygen plasma for 1 min. Following this, HFE-processable negative tone photoresist was coated with spin speed at 2000 rpm and baked 75℃ for 2 min. Following UV exposure (84 mJ/cm^2), bake (at 70 °C), and development in HFE-7500, the fluid layer (second layer) features were generated on the SU-8 patterned substrate. In this experiment, we have fabricated the polymer-based 3-D tile by using the fluorous solvent to make fluid channel in the tile. This is because fluorous solvents are poor solvents for nonfluorinated organic materials. Among the variety of fluorous solvents, segregated hydrofluoroethers (HFEs) attracted our attention because of their nonflammability noncracking, and other unfavorable physical or chemical damage of organic materials. For the third layer, another 25 μm thick SU-8 was patterned on fluid layer using the same procedures of first SU-8. To penetrate fluids into the internal channel of tile, the HFE-processable negative tone photoresist of the second layer was removed by HFE-7500 solvents (3M Company). After completion, the tiles were detached from the wafer with 1165 photoresist stripper (Shipley Microposit) for overnight. As can be seen from Figure 14 (which shows the actual tiles during representative stages of the fabrication process), we have been able to manufacture the successful 3-D tiles based on the SU-8 polymer.

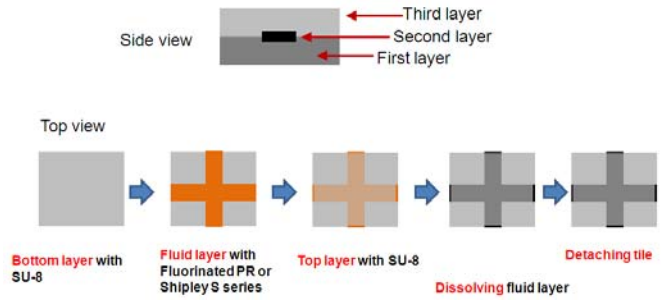

***Figure 13* – Schematic showing details of fabrication procedure developed for making the "3D" tiles with embedded microchannels.**

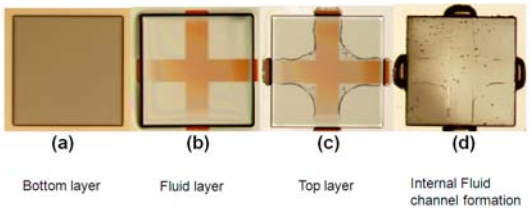

***Figure 14*–Images showing 3D tiles at various stages during the fabrication procedure.** (a) base layer deposited (b) after patterning of microchannel layer and upper substrate. (c) after hard bake of upper substrate (d) after developing of channels. The red cross in part (b) shows the location of the embedded channel.

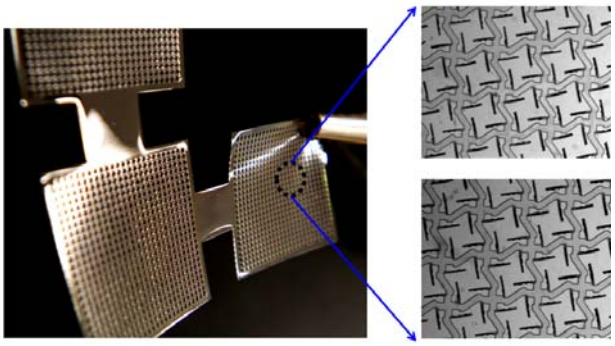

***Figure 15* – Pattern for 3D Polymer tiles with embedded microchannels and latches.**

To ensure continuity of the microchannels through the tiles we performed a series of initial dye doped fluid infusion experiments. The results of these experiments are shown in Figure 14. The image shows that the channels are indeed free, clear and leak free since the due can be seen to infuse through the structure tracking out only the microchannels. The major challenges with the 3D tiles that we will tackle in the short term are: increasing the channel height (the current height is only 2.5μm and thus the flow through them is relatively slow), releasing them from the substrate (we do not expect that release will be difficult but we have not accomplished it yet) and dispersing them in solution (we have demonstrated this with the silicon tiles but are unsure of how the polymer tiles will be behave). In addition to the above we have also fabricated a series of polymer tiles with different latching mechanisms as shown in Figure 15. We will begin experimentation with these tiles in parallel with those to be conducted using the flow through tiles.

ACKNOWLEDGEMENTS

This work was supported by the Defense Sciences Office, Programmable Matter Program.

REFERENCES

1. Balazs, A.C., Emrick, T., and Russell, T.P., *Nanoparticle polymer composites: Where two small worlds meet.* Science 314: p. 1107-1110 (2006).
2. Zykov, V., Mytilinaios, E., Adams, B., and Lipson, H., *Self-reproducing machines.* Nature 435: p. 163-164 (2005).
3. Yim, M., Shen, W.M., Salemi, B., Rus, D., Moll, M., Lipson, H., Klavins, E., and Chirikjian, G.S., *Modular self-reconfigurable robot systems - Challenges and opportunities for the future.* Ieee Robotics & Automation Magazine 14: p. 43-52 (2007).
4. Moorhouse, D., Sanders, B., von Spakovsky, M., and Butt, J., *Benefits and design challenges of adaptive structures for morphing aircraft.* Aeronautical Journal 110: p. 157-162 (2006).
5. Wickenheiser, A.M. and Garcia, E., *Longitudinal dynamics of a perching aircraft.* Journal of Aircraft 43: p. 1386-1392 (2006).
6. Compton, K. and Hauck, S., *Reconfigurable computing: A survey of systems and software.* Acm Computing Surveys 34: p. 171-210 (2002).

7. Vuillemin, J.E., Bertin, P., Roncin, D., Shand, M., Touati, H.H., and Boucard, P., *Programmable active memories: Reconfigurable systems come of age.* Ieee Transactions on Very Large Scale Integration (Vlsi) Systems 4: p. 56-69 (1996).
8. Yim, M., Roufas, K., Duff, D., Zhang, Y., Eldershaw, C., and Homans, S., *Modular reconfigurable robots in space applications.* Autonomous Robots 14: p. 225-237 (2003).
9. Zhu, J.H. and Sutton, P., *FPGA implementations of neural networks - A survey of a decade of progress.* Field-Programmable Logic and Applications, Proceedings 2778: p. 1062-1066 (2003).
10. Zhang, X.J. and Ng, K.W., *A review of high-level synthesis for dynamically reconfigurable FPGAs.* Microprocessors and Microsystems 24: p. 199-211 (2000).
11. Krishnan, M., Tolley, M.T., Lipson, H., and Erickson, D., *Increased robustness for fluidic self-assembly.* Physics of Fluids 20 (2008).
12. Tolley, M.T., Krishnan, M., Erickson, D., and Lipson, H., *Dynamically programmable fluidic assembly.* Applied Physics Letters 93 (2008).
13. Krishnan, M., Park, J., and Erickson, D., *Optothermorheological flow manipulation.* Optics Letters 34: p. 1976-1978 (2009).
14. Philp, D. and Stoddart, J.F., *Self-assembly in natural and unnatural systems.* Angew. Chem. 35: p. 1155-1196 (1996).
15. Whitesides, G.M. and Grzybowski, B., *Self-Assembly at all scales.* Science 295: p. 2418-2421 (2002).
16. Winfree, E., Liu, F.R., Wenzler, L.A., and Seeman, N.C., *Design and self-assembly of two-dimensional DNA crystals.* Nature 394: p. 539-544 (1998).
17. Olenyuk, B., Whiteford, J.A., Fechtenkötter, A., and Stang, P.J., *Self-assembly of nanoscale cuboctahedra by coordination chemistry.* Nature 398: p. 796-799 (1999).
18. Rothemund, P.W.K., *Folding DNA to create nanoscale shapes and patterns.* Nature 440: p. 297-302 (2006).
19. Bowden, N., Terfort, A., Carbeck, J., and Whitesides, G.M., *Self-assembly of mesoscale objects into ordered two-dimensional arrays.* Science 276: p. 233-235 (1997).
20. Bowden, N., Arias, F., Deng, T., and Whitesides, G.M., *Self-assembly of microscale objects at a liquid/liquid interface through lateral capillary forces.* Langmuir 17: p. 1757-1765 (2001).
21. Srinivasan, U., Liepmann, D., and Howe, R.T., *Microstructure to substrate self-assembly using capillary forces.* J. MEMS 10: p. 17-24 (2001).
22. Chung, J.H., Zheng, W., Hatch, T.J., and Jacobs, H.O., *Programmable reconfigurable self-assembly: Parallel heterogeneous integration of chip-scale components on planar and nonplanar surfaces.* J. MEMS 15: p. 457-464 (2006).
23. Chung, S.E., Park, W., Shin, S., Lee, S.A., and Kwon, S., *Guided and fluidic self-assembly of microstructures using railed microfluidic channels.* Nature Mater. 7: p. 581-587 (2008).
24. Yeh, H.J. and Smith, J.S., *Fluidic Self-Assembly for the integration of GaAs Light-Emitting Diodes on Si substrates.* IEEE Photon. Technol. Lett. 6: p. 706-708 (1994).
25. Zheng, W. and Jacobs, H.O., *Shape-and-solder-directed self-assembly to package semiconductor device segments.* Appl. Phys. Lett. 85: p. 3635-3637 (2004).
26. Golosovsky, M., Saado, Y., and Davidov, D., *Self-assembly of floating magnetic particles into ordered structures: A promising route for the fabrication of tunable photonic band gap materials.* Appl. Phys. Lett. 75: p. 4168-4170 (1999).
27. Tanase, M., Silevitch, D.M., Hultgren, A., Bauer, L.A., Searson, P.C., Meyer, G.J., and Reich, D.H., *Magnetic trapping and self-assembly of multicomponent nanowires.* J. App. Phys. 91: p. 8549-8551 (2002).
28. Glotzer, S.C., Solomon, M.J., and Kotov, N.A., *Self-assembly: From nanoscale to microscale colloids.* Aiche Journal 50: p. 2978-2985 (2004).
29. Li, Y.G., Tseng, Y.D., Kwon, S.Y., D'Espaux, L., Bunch, J.S., McEuen, P.L., and Luo, D., *Controlled assembly of dendrimer-like DNA.* Nature Mater. 3: p. 38-42 (2004).
30. Yan, H., Park, S.H., Finkelstein, G., Reif, J.H., and LaBean, T.H., *DNA-templated self-assembly of protein arrays and highly conductive nanowires.* Science 301: p. 1882-1884 (2003).
31. Chen, H.L., Schulman, R., Goel, A., and Winfree, E., *Reducing facet nucleation during algorithmic self-assembly.* Nano Lett. 7: p. 2913-2919 (2007).
32. Murata, S., Kurokawa, H., and Kokaji, S. *Self-assembling machine*. in *Proc. IEEE International Conference on Robotics and Automation (ICRA94)*. San Diego, CA (1994).
33. White, P., Kopanski, K., and Lipson, H. *Stochastic self-reconfigurable cellular robotics*. in *Proc. IEEE International Conference on Robotics and Automation (ICRA04)*. New Orleans, LA (2004).
34. Griffith, S., Goldwater, D., and Jacobson, J.M., *Robotics - Self-replication from random parts.* Nature 437: p. 636-636 (2005).
35. Goldstein, S.C., Cambell, J.D., and Mowry, T.C., *Programmable Matter.* Computer 38: p. 99-101 (2005).
36. Klavins, E., *Programmable Self-Assembly.* IEEE Control Systems Magazine 27: p. 43-56 (2007).
37. Krishnan, M., Tolley, M.T., Lipson, H., and Erickson, D., *Hydrodynamically Tunable Affinities for Fluidic Assembly.* Langmuir 25: p. 3769-3774 (2009).